Scalable Computing: Practice and Experience, ISSN 1895-1767, http://www.scpe.org
© 2024 SCPE. Volume 25, Issues 2, pp. 1029–1039, DOI 10.12694/scpe.v25i2.2523

BREAST CANCER IMAGE CLASSIFICATION BASED ON ADAPTIVE INTERPOLATION APPROACH USING CLINICAL DATASET

SUSMITHA UDDARAJU[*], A KOUSALYA[†], I HEMALATHA[‡], M MARAGATHARAJAN[§], C BALA SUBRAMANIAN[¶] AND L SATHISH KUMAR[‖]

Abstract. In the healthcare and bioinformatics disciplines, the categorization of breast cancer has become an emerging paradigm due to the second most common cause of cancer-related mortality in women. A biopsy is a procedure in which tissue has been examined to determine whether or not it is breast cancer through histopathologists that may lead to a mistaken diagnosis. The research is mainly focused on the patient data (884 case reports of patients) is acquired from the American Oncology Institute implemented with preprocessing techniques consists of missing values and those values are recovered with Novel Modified Interpolation (MI) Method. Deep learning networks effectively detect and assess the pattern for annotating histological data based on the labelling, which preserves time, system cost and enhances the system accuracy. This framework addressed feature acquisition and missing analysis strategies based on entropy confidence weight factor. First, the iterative patterns have been treated as a potential diagnostic rule, and the attention-based rule combination formulates the classification issue based on integrating convolutional and recurrent neural networks, and the short-term and long-term spatial correlations between patches. Second, the key part of label construction is carried out with an entropy confidence-weight factor assessment which detects and predict different patterns to construct the rule for classification. Third, optimization of clustering data by assessing missing parameters based on mean square error and the concept of interpolation to reduce data loss by around 20% and enhance the system accuracy. Simulation results show that the proposed system achieves 91.3% accuracy to state-of-art approaches, potentially allied in clinical applications. Modified Interpolation (MI) method recovered missing values with least mean square error and less data loss of 0.0123 and 1.38% respectively. This method also compared with existing Linear Interpolation (LI) method which is able to recover least men square error and data loss of 3.295 and 18.925% respectively. Comparatively the modified interpolation method recovered the missing values with less mean square error and less data loss.

Key words: Breast Cancer, attention-based rule combination, Data Classification, Breast Cancer Diagnose, Data Clustering and Recovery

1. Introduction and examples. Breast cancer is the second leading cause of death in women, behind lung cancer, and it is the most frequent and lethal invasive cancer in women. According to the WHO's International Agency for Research on Cancer (IARC), 8.2 million people died in 2012 due to cancer-related causes. By 2030, experts predict that the number of new cases will have risen to almost 27 million [1]. Based on apparent signs, particularly in past decades, doctors have been keeping track of lumps since they may develop into tumours. It is true since breast lumps often appear as outwardly apparent tumours in contrast to other forms of cancer inside the body. Early discovery and diagnosis were difficult since the disease was stigmatized by social stigma and shame. In addition to medical periodicals and novels, literature seldom mentioned breast cancers. The involvement of women in active promotion and awareness is essential to mitigate this impact. Chemotherapy is a medicinal treatment that uses strong chemicals to control the disease but that damage body fast-growing cells. Chemotherapy is the regularly utilized disease therapy since disease cells develop and multiply altogether quicker than the other body's cells. Chemotherapy meds arrive in different structures. Chemotherapy drugs can treat a great many malignancies, either alone or in blend. Chemotherapy is a powerful

[*]Department of Computer Science and Engineering, Koneru Lakshmaiah Education Foundation, Vaddeswaram, Guntur Dist., AP, India (susmithauddaraju@gmail.com).
[†]Department of Information Technology, Sri Krishna Collage of Engineering and Technology, Coimbatore, Tamilnadu, India (kousalyaa@skcet.ac.in).
[‡]Department of Information Technology, S. R. K. R. Engineering College, Bhimavaram, India (indukurihemalatha@ gmail.com).
[§]VIT Bhopal University, Kothrikalan, Madhya Pradesh, India (maragatharajanm@gmail.com).
[¶]Department of Computer Science and Engineering, Kalasalingam Academy of Research and Education, Srivilliputhur, Tamilnadu, India (baluece@gmail.com).
[‖]VIT Bhopal University, Kothrikalan, Madhya Pradesh, India (lsathishkumarsva@yahoo.in).

therapy for some kinds of disease, yet it likewise accompanies a gamble of unfriendly impacts.

Every year on October 19, people around the world observe International Breast Cancer Day of Awareness to raise awareness of breast cancer. For women, breast cancer makes up close to 30% of tumors. The objectives of World Breast Cancer Day 2022 are to increase awareness and support women's access to prompt and efficient prevention, detection, and treatment. Total number of 87,090 female died from Breast Cancer in the year of 2018 alone in India which is also represented in Fig. 3.1. Breast Cancer accounted for about 24.5% of all cancer related deaths in women in India [2].

Almost about one in four deaths due to cancer, in ladies in our country, was due to Breast Cancer. Mortality Rate of Different Cancer Patients [3] Once the patient diagnosed with breast cancer, the anticipated progression and outcome of your ailment will be estimated by the doctor. The prognosis varies from person to person and depends on a no of variables, like age of the patient, region of the patient, grade, and extent of the cancer. As you become older, your risk of getting breast cancer rises. women between the ages of 65 and 74 are the 2 ones who are diagnosed with breast cancer most frequently. Reliable Source. The median age that women are given breast cancer diagnoses is 63 years old. Less than 2% of the ladies in our country who received a BC diagnosis between 2015 and 2019 were under the age of 35.

Some chemotherapy incidental effects are minor and controllable, while others can life-compromise. In recent years, histopathological image usage and analysis accuracy has been increased due to the deployment of deep learning approaches. However, there are certain issues with deep learning approaches as follows:

1. Size of image data and high time consumption to train the data.
2. Computationally expensive when feeding raw data.

Few recent works have achieved moderate accuracy by stochastic selection of patches from image [2] or resizing the images [3, 4], but both mechanisms are affected by abnormal information loss that could lead to misdiagnosis. Histopathological image classification (HIC) assess different types of lesions (such as benign and malignant tumours). In [2], a sparsity model has been designed to encode image patches based on a fusion of attention patch predictions. Segmentation of the Whole side image (WSI) patch is essential during cancer image classification, and this segmentation would be into blocks and super-pixels based on the HIC approach. Consequently, the content-based histopathological image retrieval (CBHIR) method probes regions with similar content towards ROI. This mechanism provides comprehensive information to classify the images and helps pathologists. CBHIR provides comprehensive information for effective diagnosis based on historical data analysis. As per the studies, CBHIR has achieved similar accuracy compared to HIC [19]. The CNN extract the features of each patch where a support vector machine (SVM) is utilized to classify histopathological image [5]. Usually, the histopathological image classification process splits the image into smaller patches; the CNN based patch classification results are used to classify the cancer image. Histopathological image resolutions sometimes cause adverse effects that may impact the accuracy due to ignoring long-distance spatial dependency. Sometimes, the feature patch selection is not prosperous because of significant data loss that leads to insufficient data fusion. Subsequently, there are few research challenges with open-source data sets like ImageNet for object detection, BreaKHis dataset [18] and Bioimaging2015 dataset [7]. However, their diversity is not guaranteed. In this regard, the designed method assesses the multilevel features based on the patches' long and short-term spatial correlations. Second, the label construction is carried out with an entropy confidence-weight factor assessment which detects and predict different patterns to construct the rule for classification. Third, optimization of clustering data by assessing missing parameters based on mean square error and the concept of interpolation to reduce data loss. Finally, the RNN is deployed to fuse the patch features for final image classification. The 4-class classification task would achieve an accuracy of 91.3% than state-of-the-art methods. The proposed strategy is quicker and effective than the extant strategies. The usage can be considered as an augmentation of a medical clinic arrangement to monitor patient status distantly. Our contributions are listed below:

1. Design a attention-based rule combination to construct potential diagnostic rule for classification issue formulation.
2. Design an entropy confidence-weight factor to detects and predict different patterns prior to classification.
3. Design an optimization strategy to optimize clustering data loss based on mean square error and

interpolation to enhance the system accuracy.

The rest chapter is compiled as: Section 2 describes related work with respective to feature extraction and its issues. Section 3 describes proposed method and attention-based rule combination scheme for effective classification. Section 4 describes implantation and results analysis. Section 5 describes conclusion of the manuscript.

2. Related Work. Many scientific domains rely on spatial and biological interpolation of spatio temporal and socioeconomic data. Nearest neighbour (NN), inverse distance weighting (IDW) [8], and trend surface mapping (TS) [9] are some basic interpolation approaches. Geostatistical interpolation (kriging) [10] was introduced in the 1980s. Because kriging considers spatial correlation and quantifies interpolation error using the kriging standard deviation, this was a significant improvement.

Under unambiguous stationarity suspicions, In spatial information kriging is the Best Linear Unbiased Predictor (BLUP)[11]. It is also relatively adaptable, as numerous variations can handle specific situations like anisotropy, non-normality, and information included in covariates [12].

Kriging, on the other hand, has drawbacks. It can be computationally intensive, and it might be challenging to develop a solid geostatistical model that effectively fits all sorts of data [13]. It is also not well suited to adding the vast amounts of covariate data that are now available. One significant challenge is that defining a geostatistical model for data that cannot be easily transformed to normalcy is difficult. Indicator kriging [14] was created to address this problem; however, it is badly designed and not model-based (i.e., it doesn't utilize formal factual strategies inferred for an unequivocal and complete measurable model, see Diggle and Ribeiro). The Summed up Direct Geostatistical Model [15] is statistically solid, but it has limitations regarding the types of distributions it can handle, and it is also technically challenging. For example, it is not always clear how variables with a lot of them interact.

Despite the fact that yearly and month to month precipitation in arid regions can in any case have zero qualities and solid positive skewness, spatial addition utilizing kriging is less complicated than every day or hourly precipitation in light of the fact that transiently collected precipitation keeps an eye on the typical dissemination[6]. However, when mapping hourly or daily precipitation, geographic variability is more significant, the stationarity assumption is called into question, and the precipitation distribution becomes skewed and filled with zeros [16]. From the literature, it is clear that there is a need for an extensive database to do adequate research. That cluster's data must be omitted if even one parameter is missing. Usually, 20% of the data may be missed because of a single missing parameter in the database. We designed an algorithm to recover missing parameters with a small mean square error to prevent this problem. The designed method assesses the multi-level features based on the patches' long and short-term spatial correlations. Second, the label construction is carried out with an entropy confidence-weight factor assessment which detects and predict different patterns to construct the rule for classification [17]. Third, optimization of clustering data by assessing missing parameters based on mean square error and the concept of interpolation to reduce data loss. At long last, the RNN is sent to combine the fix highlights for definite picture order.

3. Proposed system. Fig. 3.2 represents the Steps to perform and apply MI method as below:

1. Clustering of database.
2. Define overlap clustering for different classes.
3. Locate the cluster with missing parameters.
4. Apply modified interpolation to recover missing parameter.

Firstly, the collected real time data is clustered because the collected data is independent, we have to consider the classes. So we cluster our data by using output feature. Secondly, have to consider overlap clustering because there are many different classes, by using that classes that any data is overlapping. Thirdly, location of cluster with missing parameter is done to apply MI method. Once the location of the cluster is founded the MI model is applied to recover missing value.

The clustering approach is formulated based on spatial correlations, feature and instance dimension in a matrix format. Let assume m $\times$ n matrix A, and matrix B is sub-set of matrix A; where m is number of rows refers cases, n is number of columns refers features. The tumors have assigned scores to identify the lesion type for breast tumour diagnosis. In most cases, the score based analysis is not optimal; therefore, constant features have considered to accomplish the image classification. The mean-square-residue score (MSRS) measures each

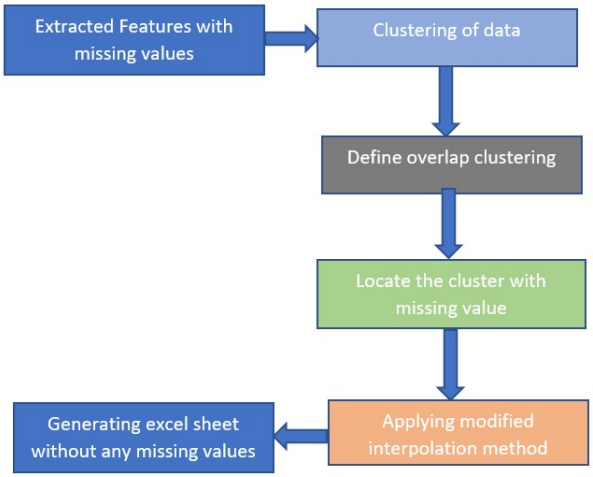

Fig. 3.1: Flowchart of recovering missing values.

Table 3.1: Tumor characteristics.

Characteristics of	**benign**	**malignant**
Shape	Oval	Irregular
Orientation	Parallel	Non-parallel
Border	distinct	indistinct
Margin	without spiculated	spiculated

cluster's rate during the image classification. Each cluster enables at least 5 rows to formulate the unique rule in our simulation.

Initializes the required parameters, such as probability error and supportive confidence weight attributes. Step 1: check all image patches to construct the rule based on a cluster with an influential confidence factor. step-3 define the parameters, line-4 estimates the distance threshold value. step-6 to step-7 construct the cluster when the MSRS score is less than its threshold value. Otherwise, go to step-2, and this process is repeated till the construction of the cluster with an optimal confidence value. The final cluster remains used to construct the diagnosis rule, but there is a need to assess the confidence factor to validate the reliability. The rule construction must differentiate benign or malignant categories. Let us assume, K_{be} indicates benign-label rows, K_{ma} indicates malignant-label rows and K_{bm} indicates total rows of a cluster. The confidence-weight factor ϕ is derived as follows

$$\phi_{be} = \frac{K_{be}}{K_{bm}} \tag{3.1}$$

$$\phi_{ma} = \frac{K_{ma}}{K_{bm}} \tag{3.2}$$

The essential confidence-weight factor ϕ of image g or cluster is derived as follows

$$\phi_g = \max\{\phi_{be}, \phi_{ma}\} \tag{3.3}$$

The cluster is classified based on the larger confidence-weight factor ϕ. The cluster-based rule construction is conditionally formulated when the satisfaction of this condition $\phi \geq \phi_{th}$. In our simulation, the $\phi_{th}$is fixed with 0.75 to enhance the system accuracy.

Algorithm 1 Pseudocode of spatial correlation method

Input: Collected data with missing values in the form of Excel
Read the excel sheet
Initialize an empty array called 'missingElements'
for each column in excel sheet:
if column name is 'No of Missing Values':
value of cell > 0:
add this row to 'missingElements' array
Initialize a data structure 'D'
for storing clusters for each element in 'missingElements' array:
pass the element to the Mathematical model:
use KNN clustering to form clusters consecutively C_1, C_2, C_3... and store in D
for each cluster C_i in D:
for each feature F_j in C_i:
for each value P_k in F_j:
$\sum P$: Sum of values Pk in the feature F_j
PN: Number of missing values in feature F_j
P*: missing value
Define Overlap Clustering for the above formed clusters and missing values.
Locate the cluster with missing values.
Apply Modified interpolation method to remove missing values.
Output: Generates new excel sheet by recovering missing value

Computer-aided pathology analysis relies on the ability to classify breast cancer data. The researcher proposes to use a modified interpolation technique with data clustering to identify missing characteristics in a breast cancer database. In this regard, first extracting useful and non-redundant characteristics that are not redundant.

Let us assume, $Database \in \{C_1, C_2, \cdots, C_N\}$ enables N set of clusters and each cluster is constructed based on set of features F_N such as $C \in \{F_1, F_2, \cdots, F_N\}$ and each feature is extracted based on set of parameters such as $F \in \{P_1, P_2, \cdots, P_N\}$. Now he missing parameters are derived as follows

$$\hat{P} = \frac{\sum \frac{\partial P}{\partial F} + \sum P}{P_N} \tag{3.4}$$

where $\frac{\partial P}{\partial F}$ is a derivative parameter of the concern feature. All possible combinations have been performed on the target variables. The nearest location is first calculated for the calibration. The map of the nearest calibration variables is then fed to the gradient calculation. The missing parameter equation is used to find out the nearest prediction parameters as shown in the proposed system architecture. During HIC, the object may have different scales and complexity that leads hard to characterize image features. In this regard, CNN has achieved high accuracy, but the HIC requires excellent attention to represent the features. Therefore, combining multi-layer features helps to achieve the targeted accuracy by retaining fine-grained details and local textures, as we can observe in Fig. 3.3. The Tensorflow slim distribution helps to assess the feature extraction. In our simulation, the fully connected layers have not been considered due to the arbitrary size of images. Each layer channel is combined to accomplish multilevel convolutional features based on global average pooling with two inception modules. The final vector with 4096D dimensions enable multi-features of the image to classify the breast cancer images.

4. Experiment Result Analysis. Using the Tensor Flow framework the proposed algorithm is executed. The CNN architecture is a basic deep model, an AlexNet is employed as pre-trained model on the ImageNet. The essential settings of the server incorporate an Intel 3.6-GHz CPU and NVIDIA GeForce GTX 1080Ti GPU. In this periment, 1062 breast cancer instances (418 benign, 644 malignant cases) are considered. The SVM, fuzzy SVM, GRNN based methods are considered as state-of-art approaches. Fig. 4.1 illustrates different tissue

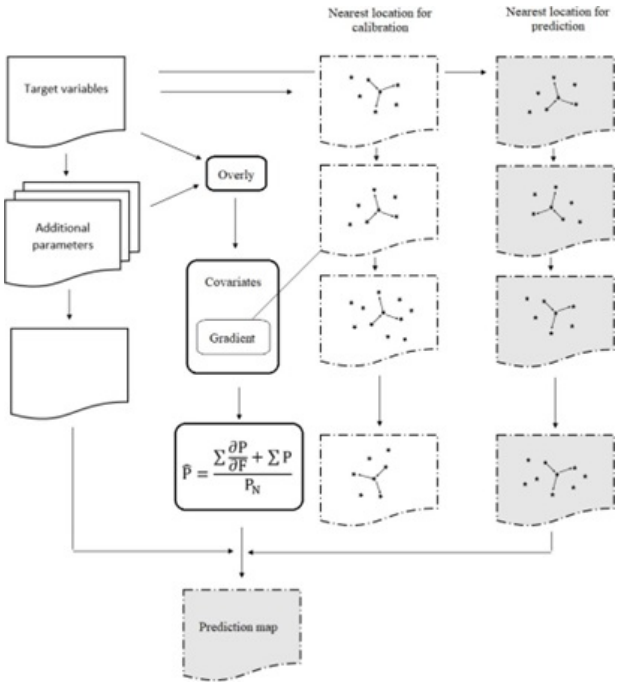

Fig. 3.2: Proposed System Architecture

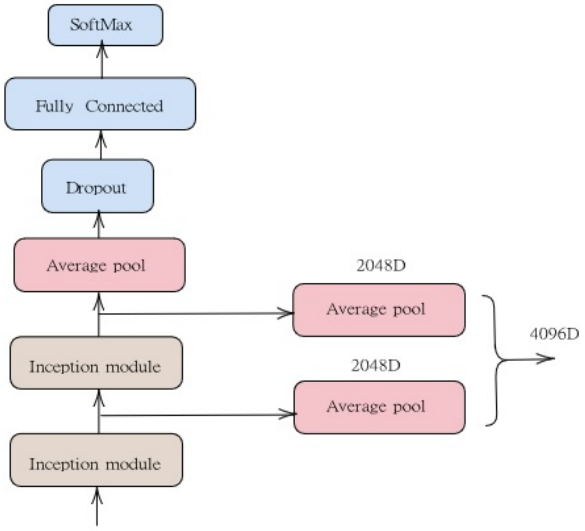

Fig. 3.3: Schematic overview of feature representation

samples which considered as classes to assess the performance of the system, and where a) is a normal tissue, b) is a benign tissue, c) is a In-situ carcinoma, d) is a Invasive carcinoma.

4.1. Performance Metrics. Distinctive execution measurements are used to decide the productivity of our approach. Well known system performance like Accuracy, sensitivity and specificity are measured. The

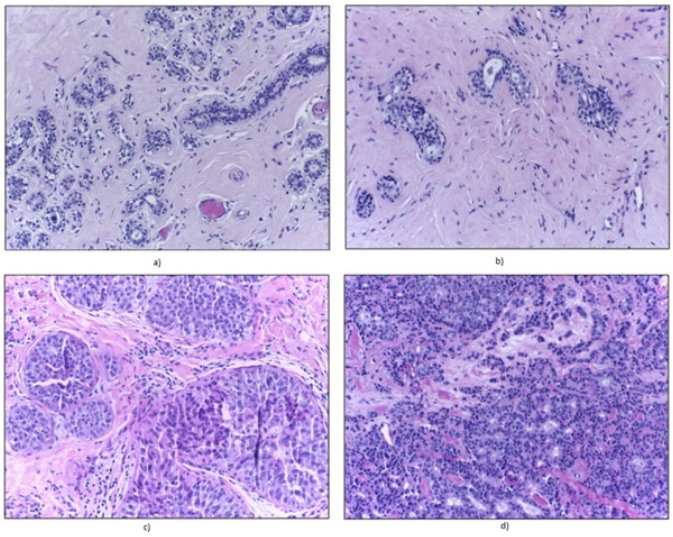

Fig. 4.1: Four different tissue samples

Table 4.1: Classification based on essential attributes.

S.No	ML Model	-1,1	-1,1	-1,1	TP	TN	FP	FN	Acc	TPR	TNR	FPR	FNR	PPV	NPV
1	SVM	138	54	28	138	536	54	28	89.15	83.13	90.85	9.15	16.87	71.88	95.04
2	GRNN	192	0	564	192	100	0	564	34.11	25.4	100	0	74.6	100	15.06
3	Fuzzy SVM	125	67	11	125	553	67	11	89.68	91.91	89.19	10.81	8.09	65.1	98.05
4	DL-AI approach	171	24	4	171	567	24	4	96.1	97.01	95.11	3.95	1.74	86.21	99.41

accuracy is the proportion of correct classification in all instances. The sensitivity is the proportion of positives (malignant instances) that are correctly identified, and the specificity is the proportion of negatives (benign instances) that are correctly identified, which are are listed below.

$$\Pr ecision = \frac{(TP)}{(TP) + (FP)} \tag{4.1}$$

$$Accuracy = \frac{(TP) + (TN)}{((TP) + (TN)) + ((FP) + (FN))} \tag{4.2}$$

$$MAE = \frac{1}{N} \sum_{i=1}^{N} \|P_i - Q_i\| \tag{4.3}$$

Exactness speaks average capacity of DRL model. True positive (TP) and true negative (TN) measure concludes the nonappearance and nearness of C-19 virus. False positive (FP) and false negative (FN) recognize the quantity of bogus caused by the system. Function measure (FM) remain used to decide the expectation execution rate. Root mean square error (RMSE), mean absolute error (MAE) have used to assess distinction rate among real and anticipated esteems. Table 4.1 illustrates that our DL-AI approach has achieved reasonable accuracy than other extant approaches. The precision rate is stable and DL-AI approach accomplished tremendous precision than the extant models because the designed Spatial Co-relation system effectively classify the images based on DRL system.

Table 4.2: Comparative analysis of proposed method with other models.

Study	Feature Extraction	Classifier Method	Classes	Accuracy (%)
1	WT	SVM	3	89.1
2	Morphology	GRNN	5	88.5
3	Floating Features	Fuzzy SVM	5	90
4	Spatial Co-relation	DL-AI approach	5	91.3

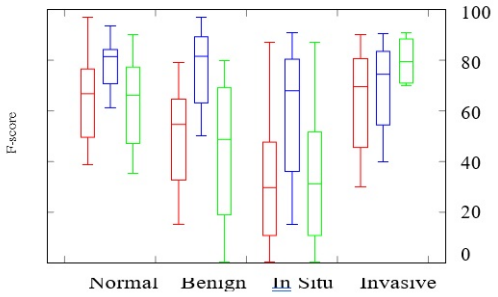

Fig. 4.2: F-Score comparative analysis

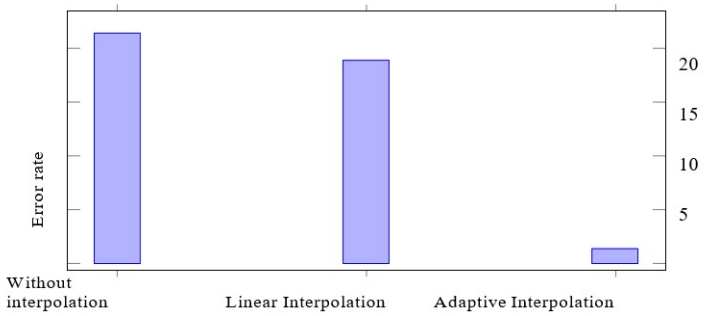

Fig. 4.3: Error rate analysis and without interpolation

Table 4.2 illustrates comparative analysis of proposed method with state-of-art approaches. Five different classes are considered to assess the accuracy of the system and the proposed system has achieved 91.3% accuracy than other approaches. Fuzzy-SVM model has also achieved notable accuracy which is around 90%.

Fig. 4.2, illustrates F1-score with box-plots of the proposed and state-of-art approaches over test set. All approaches have accomplished the most elevated F1 esteems due to effective clustering based on weight factor. The DL-AI approach has achieved essentially accurate outcomes for all test cases. Most researchers have used a modified interpolation technique for weight assessment and the KNN algorithm for data clustering to identify missing characteristics in a breast cancer dataset. Fig. 4.3 illustrates performance analysis of a proposed system with and without interpolation; the model without interpolation has achieved an average 21% error rate compared to linear interpolation. However, adaptive interpolation has achieved leq5% error rate on average. The cluster has omitted if any of the parameters are mismatched and when the confidence weight factor value is insufficient.

Initial simulation is carried out with normal and abnormal tissue data-set which can be observe in Fig. 4.4. Compare to GRNN, DL-AI has achieved high performance rate than FSVM in terms of accuracy 97% and sensitivity 98.3%, and specificity is 94% respectively. FSVM has occupied second position in performance rate but the specificity is 91% which is greater than GRNN. The GRNN has achieved 95% accuracy, 98.3%

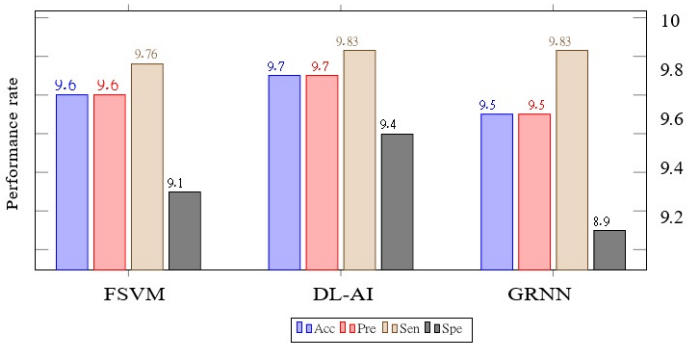

Fig. 4.4: Simulation-1 with normal and abnormal tissues

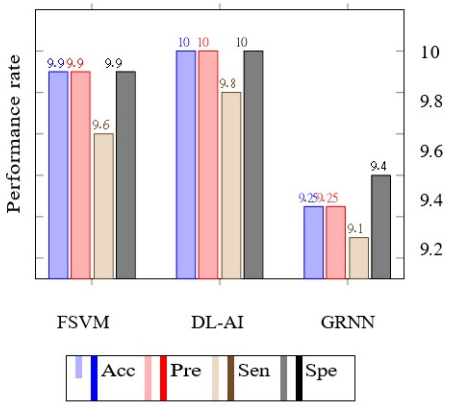

Fig. 4.5: Simulation-2 with benign and malignant

sensitivity, 89% specificity respectively.

Subsequently, Fig. 4.5 illustrates the simulation-2 results with benign and malignant tissue data. DL-AI approach has achieved grater performance than state-ofo-art approaches, like 100% accuracy, 98% sensitivity, and 100% specificity. However, GRNN has achieved low performance rate with the same tissue data set, were 92% accuracy, 91% sensitivity, 94% specificity are measured respectively. As usual, FSVM has holed the second position which is better than GRNN.

Consequently, Fig. 4.6 illustrates simulation-3 result analysis report with invasive and in situ carcinoma tissue data. Here, FSVM has achieved low performance rate than GRNN such as 91% accuracy, 90% sensitivity, 92% specificity, but GRNN has achieved 92.5%, 91%, 93% rate to wards accuracy, sensitivity, and specificity respectively. DL-AI has achieved its notable accuracy by 92%, 90% sensitivity, and 94.7% specificity respectively.

Table 4.3 illustrates standard deviation(SD), Area Under the Curve (AUC) measurement values to assess the performance of the system. In experiment-1, 500 normal and abnormal images are considered to estimate the SD, AUC based on three listed classifiers. Where, FSVM, GRNN, DL-AI have achieved 0.07%,0.05%,0.11% SD respectively. In experiment-2, FSVM, GRNN, DL-AI classifiers have achieved 0.19%,0.11%,0.21% of SD, and 0.97%, 0.99%, 1% of AUC respectively. Subsequently, this second simulation is carried out with 400 benign and malignant tissue data set. In experiment-3, FSVM, GRNN, DL-AI classifiers have achieved 0.15%, 0.163%, 0.20% of SD, and 0.98%, 0.967%, 0.99% of AUC respectively. In all three cases, DL-AI approach has achieved high performance rate than other approaches with different data-sets.

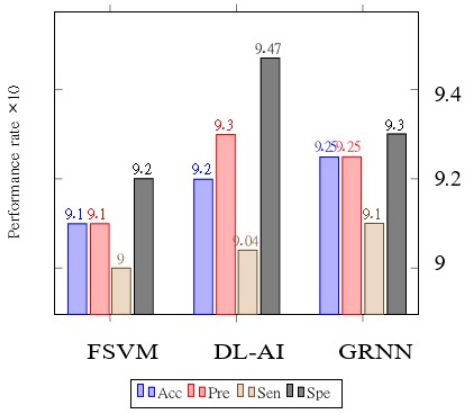

Fig. 4.6: Simulation-2 with invasive and in situ carsinoma

Table 4.3: Simulations results analysis with AUC and SD based on each classifier.

Experiment	Number of images	Classifier	AUC	SD
1	500	FSM	0.99	0.07
		GRNN	1	0.05
		DL-AI	0.99	0.11
2	400	FSM	0.97	0.19
		GRNN	0.99	0.11
		DL-AI	1	0.21
3	300	FSM	0.98	0.15
		GRNN	0.967	0.163
		DL-AI	0.99	0.2

5. Conclusion. The proposed system effectively determines breast cancer-based histopathology images to mitigate mistaken diagnosis. Deep learning networks accurately assessed the patterns for annotating histological data with a label system that enhances the system accuracy by 91.3%. The feature acquisition and missing analysis strategies have played an essential role in strategically achieving the targeted accuracy based on the entropy confidence weight factor. The attention-based rule combination effectively formulated the classification issue by detecting and predicting the different patterns to construct the classification rule. This process has optimized the clustering data by assessing missing parameters based on mean square error and data interpolation.

Note: KNN algorithm has been used during data clustering considering the above essential factors.

Simulation results show that the proposed system has achieved 91.3% accuracy than state-of-art approaches.

REFERENCES

[1] Heather D Couture, Lindsay A Williams, Joseph Geradts, Sarah J Nyante, Ebonee N Butler, JS Marron, Charles M Perou, Melissa A Troester, and Marc Niethammer, *Image analysis with deep learning to predict breast cancer grade, ER status, histologic subtype, and intrinsic subtype*, in NPJ breast cancer, 4(1), 2018, pp. 30.

[2] Mai Bui Huynh Thuy and Vinh Truong Hoang, *Fusing of deep learning, transfer learning and gan for breast cancer histopathological image classification*, in International Conference on Computer Science, Applied Mathematics and Applications, 2019, pp.255–266.

[3] Zixiao Lu and Zhan, *Brcaseg: a deep learning approach for tissue quantification and genomic correlations of histopathological images*, in Genomics, proteomics & bioinformatics, 2021.

[4] Pin Wang, Pufei Li, Yongming Li, Jiaxin Wang, and Jin Xu, *Histopathological image classification based on cross-domain deep transferred feature fusion*, in Biomedical Signal Processing and Control, 68:102705, 2021.

[5] Andreas Holzinger, Bernd Malle, Peter Kieseberg, Peter M Roth, Heimo Mu¨ller, RobertReihs, and Kurt

Zatloukal, *Towards the augmented pathologist: Challenges of explainable ai in digital pathology*, arXiv preprint arXiv:1712.06657, 2017.

[6] Uddaraju, Susmitha, GP Saradhi Varma, and M. R. Narasingarao, *Prediction of NAC Response in Breast Cancer Patients Using Neural Network*, in Scalable Computing: Practice and Experience 23.4, 2022, pp: 211–224.

[7] Scotty Kwok, *Multiclass classification of breast cancer in whole-slide images*, in International conference image analysis and recognition, Springer, 2018, pp: 931–-940.

[8] Francisco Manuel Gasca-Sanchez, Sandra Karina Santuario-Facio, Roc´io Ortiz-L´opez, Augusto Rojas-Martinez, Gerardo Manuel Mej´ia-Vel´azquez, Erick Meinardo Garza-Perez, Jos´e Ascenci´on Hern´andez-Hern´andez, Rosa del Carmen L´opez-S´anchez, Servando Cardona Huerta, and Jesu´s Santos-Guzman, *Spatial interaction between breast cancer and environmental pollution in the monterrey metropolitan area*, in Heliyon, 7(9):e07915, 2021.

[9] Lorena Consolino, Pietro Irrera, Feriel Romdhane, Annasofia Anemone, and Dario Livio Longo, *Investigating plasma volume expanders as novel macromolecular mri-cest contrast agents for tumor contrast-enhanced imaging*, in Magnetic Resonance in Medicine, 86(2), 2021, pp: 995–- 1007.

[10] Chaosheng Zhang, Renguang Zuo, Yihui Xiong, Xun Shi, and Conan Donnelly, *Gis, geostatistics, and machine learning in medical geology*, in In Practical Applications of Medical Geology, Springer, 2021, pp: 215–-234.

[11] Abbas Tavassoli, Yadollah Waghei, and Alireza Nazemi, *Comparison of kriging and artificial neural network models for the prediction of spatial data*, in Journal of Statistical Computation and Simulation, 2021, pp: 1-–18.

[12] Uddaraju, Susmitha, and M. R. Narasingarao, *Predicting the Ductal Carcinoma Using Machine Learning Techniques—A Comparison*, in Journal of Computational and Theoretical Nanoscience, 16.5-6, 2019, pp: 1902–1907.

[13] Xiaoling Leng, Rexida Japaer, Haijian Zhang, Mila Yeerlan, Fucheng Ma, and Jianbing Ding, *Relationship of shear wave elastography anisotropy with tumor stem cells and epithelialmesenchymal transition in breast cancer*, in BMC Medical Imaging, 21(1), 2021, pp: 1–16.

[14] K Venkata Ratna Prabha, D Vaishali, Pallikonda Sarah Suhasini, K Subhashini, and P Ramesh, *Different diagnostic aids and the improved scope of establishing early breast cancer diagnosis*, In Micro-Electronics and Telecommunication Engineering, Springer, 2021, pp: 65–72.

[15] Laila Al-Qaisi, Mohammad A Hassonah, Mahmoud M Al-Zoubi, and Ala'M Al-Zoubi, *A review of evolutionary data clustering algorithms for image segmentation*, In Evolutionary Data Clustering: Algorithms and Applications, 2021, pp: 201–214.

[16] Maram Alwohaibi, Malek Alzaqebah, Noura M Alotaibi, Abeer M Alzahrani, and Mariem Zouch, *A hybrid multi-stage learning technique based on brain storming optimization algorithm for breast cancer recurrence prediction*, In Journal of King Saud University-Computer and Information Sciences, 2021.

[17] Thomas Helland, Bjørn Naume, Steinar Hustad, Ersilia Bifulco, Jan Terje Kvaløy, Anna Bar bro Sætersdal, Marit Synnestvedt, Tone Hoel Lende, Bjørnar Gilje, Ingvil Mjaaland, et al. , *Low z-4ohtam concentrations are associated with adverse clinical outcome among early stage premenopausal breast cancer patients treated with adjuvant tamoxifen*, In Molecular oncology, 15(4), 2021, pp: 957–967.

[18] Fabio A Spanhol, Luiz S Oliveira, Paulo R Cavalin, Caroline Petitjean, and Laurent Heutte, *Deep features for breast cancer histopathological image classification*, in 2017 IEEE International Conference on Systems, Man, and Cybernetics (SMC), IEEE, 2017, pp: 1868–1873.

[19] Uddaraju, Susmitha, and M. Narasingarao, *A survey of machine learning techniques applied for breast cancer prediction*, in International Journal of Pure and Applied Mathematics 117.19, 2017, pp: 499–507.

Edited by: Polinpapilinho Katina
Special issue on: Scalable Dew Computing for Future Generation IoT systems
Received: Aug 18, 2023
Accepted: Dec 2, 2023